Energy & Environmental Science

Accepted Manuscript

ROYAL SOCIETY OF CHEMISTRY

www.rsc.org/ees

Energy & Environmental Science

COMMUNICATION

Energy Saving Electrochromic Windows by Bistable Low-HOMO level Conjugated Polymers

Haijin Shin, Seogjae Seo, Chihyun Park, Jongbeom Na, Minsu Han, and Eunkyoung Kim*

Received 00th January 20xx,
Accepted 00th January 20xx

DOI: 10.1039/x0xx00000x

www.rsc.org/ees

Energy saving electrochromic windows were established by controlling the interfacial charge transport using low-HOMO level (< -5 eV) π-conjugated polymers as bistable electrochromic films and an ionic liquid as an electrolyte. It provided a long bistability (> 90 min) at voltage-off state with a high color contrast (879 $cm^2 C^{-1}$).

The ability to control the light transmission through a window has captured intense interest in the field of energy saving windows to block out or manipulate dynamic daylight. Recently, the smart window has emerged as a transparent display to propel the color and light transmission technology into the realm of next generation displays, architectures, and transportation. There are several methods to control light transmission, including electrochemical mirrors[1] and electrochromic windows by using inorganic,[2] organic materials,[3] and π-conjugated polymers (CPs).[4] Regarding the inorganic materials, ECW based on WO_3 was the most widely studied.[2, 5] Particularly, CPs undergo reversible electrochemical optical changes with a fast response, and this process has garnered increasing interest because of their tunable electronic properties, low-voltage operation, and solution processability.[6] Of the various CPs, the electrochromic (EC) color and transmittance changes of the poly(3,4-propylenedioxythiophene) derivatives (PRs) have reached high color contrasts,[7, 8] which should be particularly useful for smart windows.

Smart windows change their transmittance according to the applied potential, to reduce overall energy spending of a building by approximately 25%. It also improves quality of life by increasing comfort levels for people inside the building.[9]

For such an electrochemical switching window, the optical memory (OM) during the voltage-off state (V-Off) is important for energy saving windows or displays. Furthermore, the OM at both the colored and transparent state under V-Off, called bistability, should be compulsory because no additional energy consumption is required to maintain the colored (dark) or transparent state. Unlike molecular EC dyes (e.g., viologens), that are typically dissolved in electrolyte media to generate an EC window (ECW), solid state CP films potentially limit the loss of OM caused by the diffusion of EC materials and dopant ions[10] to produce rather long OMs.[6, 11-15] However, the color contrast of ECWs in previous examples has been low (< 60% at absorption maxima (λ_{max})), and they require complicated processes. Although there have been many efforts, including ECWs with gel electrolytes [11, 14, 15] and EC molecules anchored with metal oxides or rotaxanes,[3, 16] the bistability of ECWs has rarely been reported, and it is a major hurdle in the smart windows and organic electronics, including displays. Moreover, the mechanisms to realize bistability in CPs are not well understood.

To achieve bistability in an ECW, it is important to control the spontaneous charge transfer that results in optical loss at V-Off. Fundamentally, the loss of OM is related to the charge transport between the interfaces in the ECW that consist of ITO/CP film/electrolyte/ITO. This spontaneous charge transfer (self-reaction) at V-Off can be described with Equation (1):

$$(Pol^*) + (A^-)_s \rightleftarrows (Pol^+ \cdot A^-)_{pol} + e^-_{ITO} \quad (1)$$

where (Pol^*) represents the active centers in the neutral CP films, which absorb visible light, $(A^-)_s$ is the counter ions of the electrolyte that is injected/ejected to maintain the electro-neutrality inside the CP films, $(Pol^+ \cdot A^-)_{pol}$ represents the transparent CP films with the counter ions, and e^-_{ITO} represents the electrons that are transported to the ITO.

The interfacial electron transfer (IET) between the ITO and CP films is highly influenced by the energy levels of the CPs [17]. Therefore, it can be hypothesized that the redox potential of the CP can be an exclusive controller of the IET. Furthermore, at the interface between the CP film and the electrolyte, the spontaneous interfacial dopant ion transport (IDT) should be blocked by the electrochemical double layer (EDL). [1]

Therefore, we explored a bistable ECW by controlling the interfacial charge transport in a CP-based device. First, the effect of the redox potential on the OM was examined to control the IET, which can be

Active Polymer Center for Pattern Integration, Department of Chemical and Biomolecular Engineering, Yonsei University, 50 Yonsei-ro, Seodaemun-gu, Seoul. 03722. South Korea. E-mail: eunkim@yonsei.ac.kr

†Electronic Supplementary Information (ESI) available: Description of materials and methods, TableS1-S4 and Fig. S1-S13. See DOI: 10.1039/x0xx00000x

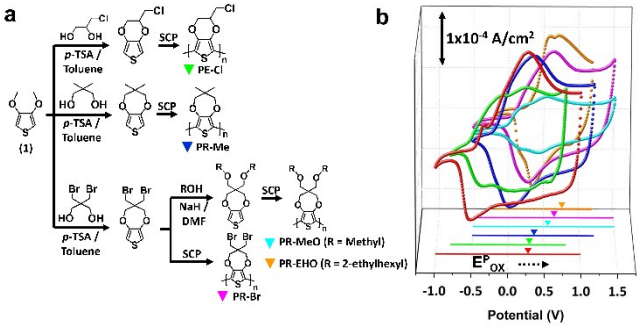

Fig. 1 (a) Synthetic routes for the monomers and polymers. (b) Cyclic voltammograms of the CPs coated on an ITO in TBAP as the electrolyte at a scan rate of 50 mV s^{-1} (vs. Ag/AgCl) for PEDOT (red), PE-Cl (green), PR-Me (blue), PR-MeO (cyan), PR-Br (magenta), and PR-EHO (orange).

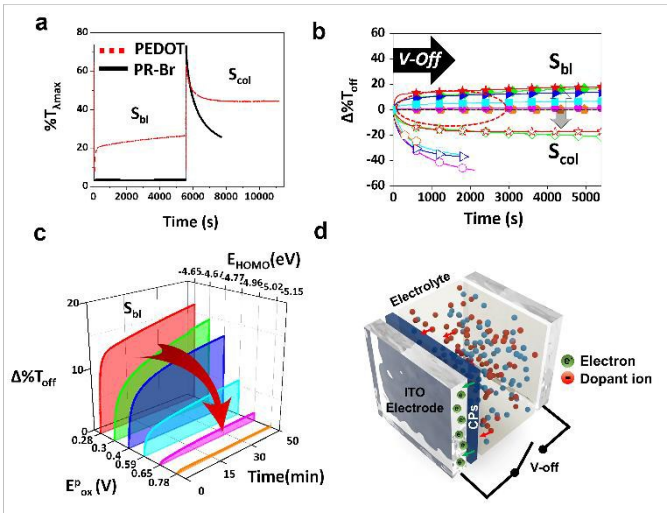

Fig. 2 (a) The transmittance change for S_{bl} and S_{col} at V-Off of an ECW for the PEDOT (dotted red line) and PR-Br (solid black line) films in TBAP and monitored at λ_{max}. (b) $\Delta\%T_{off}$ in the colored (S_{bl}, closed symbols) and bleached state (S_{col}, open symbols) for PEDOT (red star), PE-Cl (green diamond), PR-Me (blue triangle), PR-MeO (cyan square), PR-Br (magenta circle), and PR-EHO (orange pentagon). (c) A plot for $\Delta\%T_{off}$ in the colored state (dotted red circle of Fig. b) as a function of the E^p_{ox} and E_{HOMO} of the CPs. (d) A schematic diagram of the interfacial electron transport in TBAP for S_{bl}.

unfavorable when the HOMO energy level (E_{HOMO}) of the CPs is lower than the Fermi level (E_F) of the electrode.[18] Thus, a series of CPs with a different E_{HOMO} were synthesized to characterize the IET. Our structural motif was based on PRs because these can be easily chemically modified to alter their redox properties via tailor-made molecular designs and to exhibit a high color contrast. Next, the IDT was controlled by using ionic liquids[19], which form ion blocking layers through the EDLs.[1] Herein, we report a bistable electrochromic window (BECW) based on a new high color contrast PR derivative that has a low E_{HOMO}.

The ~250-nm-thick CP films were easily coated on an ITO glass via solution casting polymerization (SCP) of monomers (Fig. 1a).[20] As shown in the cyclic voltammogram (CV) (Fig. 1b), the redox potential of the PR films was highly dependent on the monomer structure and exhibited higher oxidation peak potentials (E^p_{ox}) than the poly(3,4-ethylenedioxythiophene)s (PEDOTs) in a propylene carbonate solution containing 0.1 M tetrabutylammonium perchlorate (TBAP) when using Ag/AgCl as a reference. This high E^p_{ox} for the PR films can be attributed to the large alkylenedioxy group, which decreases the planarity of the polymer main chain.[21, 22] The CPs with electron withdrawing (Cl, Br) and bulky side groups (EHO) exhibit higher E^p_{ox} because of the electronic [23, 24] and steric hinderance effect,[25, 26] respectively. The effects of the substituents on the redox potential of the CPs in an ionic liquid media that contained 1-butyl-3-methylimidazolium bis(trifluoromethylsulfonyl)imide (BIL) were nearly identical to those in the TBAP, except for PR-EHO (Fig. S1 and Table S1, ESI†). The E_{HOMO} of the CP film was estimated from the CV and was confirmed by UPS (Table 1 and Fig. S5, ESI†).

The structure of the ECW was consisted of an ITO/CP film/electrolyte/ITO. To test the optical stability, the transmittance at λ_{max} ($\%T_{\lambda max}$) of the ECW was monitored for 90 min at V-Off in both TBAP (Fig. 2a) and BIL (Fig. 3a). Interestingly, the OM of the colored states for the PR-Br and PR-EHO were superior to those of the other polymers, and the transmittance change at λ_{max} under V-Off ($\Delta\%T_{off}$) in the colored state (self-bleaching, S_{bl}) was almost negligible (< 2%) in both TBAP and BIL (Fig. S3, ESI†). However, with PEDOT, the $\Delta\%T_{off}$ in the colored state was 15% and 20% after 30 min in TBAP and BIL, respectively, and showed the highest change among the CPs (Fig. 2b and Fig. 3b). The OM in the colored state did not depend much on the electrolyte; however, it was highly dependent on the E^p_{ox} of the CPs (Fig. 2c). When the electricity was shut off in the colored state, the spontaneous optical loss could be ascribe to the IET (Fig. 2d). This IET is possible when the E_{HOMO} of the CPs is higher than the E_F of the ITO electrode (-4.7 eV).[27]

The $\Delta\%T_{off}$ of the transparent state (self-coloring, S_{col}) was larger than that of the colored state and was dependent on the CPs in TBAP. The $\Delta\%T_{off}$ of PEDOT and PE-Cl were ~20% within 30 min, which was smaller than those of the other CPs (> 40%) (Fig. 2b). However, the OM in BIL was dramatically enhanced (Fig. 3a and b), possibly because of the formation of EDLs. EDLs persist long even after the applied voltage is off, preventing interfacial ion transfer [1, 28]. Therefore, the IDT in BIL could be blocked (Fig. 3c).

The stability of the EDLs at V-Off is highly dependent on the size of the ions (Fig. S7 and Fig. S8, ESI†). The OM was shorter in BBF_4 that consisted of very small anions (BF_4^-), which may cause an imbalance between the surface counter ions and the ion-ion steric repulsion.[29] Conversely, large anions could be paired compactly with cations. Specifically, BILs have been reported to form more densely packed multi-double layers on a charged surface.[30] Therefore, all of the CPs in BIL exhibited low $\Delta\%T_{off}$ (< 10%) even after 90 min (Fig. 3b, S_{col}), in contrast to that in TBAP.

The reproducible bistability was successful in an ECW with PR-Br, exhibiting a long OM at V-Off in the colored and bleached state (Fig. 4a and b). The cyclability of ECW was longer than 500 cycles in air (Fig. S4, ESI†). A larger-area ECW (7 inch) was also fabricated and achieved a high color contrast and a long OM (Fig. 4c).

In the colored state, the electron transfer from the CP films to the electrode is spontaneous if the E_F of electrode is below the E_{HOMO} of

Table 1 Electrochemical properties of the CPs.

CPs	E^p_{red} [V] [a]	E^p_{ox} [V] [b]	$E_{1/2}$ [V] [c]	E_{HOMO} [eV] [d]	E_{LUMO} [eV] [e]	E_g [f]
PEDOT	-0.52 (-0.6[31])	0.28 (0.01[31])	-0.12	-4.65	-2.98	1.67 (1.6~1.7[10])
PE-Cl	-0.42	0.3	-0.06	-4.67	-3.02	1.65
PR-Me	-0.18 (-0.3[31])	0.4 (0.03[31])	0.11	-4.77	-2.9	1.87
PR-MeO	0.16	0.59	0.38	-4.96	-3.14	1.82
PR-Br	0.14	0.65	0.40	-5.02	-3.19	1.83
PR-EHO	0.17 (0.08[26])	0.78 (0.25[26])	0.48	-5.15	-3.21	1.94 (1.97[10])

[a, b] E^p_{red} and E^p_{ox} are based on the Bigaussian multi-peak deconvolution of the cyclic voltammogram in TBAP, which was used as the electrolyte, vs. Ag/AgCl. [c] Half-wave potential. [d] The E_{HOMO} was calculated by using E^p_{ox} and estimated with the empirical relation $E_{HOMO} = -4.8e - e[E^p_{ox} - E_{1/2\ Ferrocene}]$ [e] E_{LUMO} of the CPs, as determined from the E_{HOMO} and E_g of the CPs. [f] E_g of the CPs, as determined from the onset of the π-π* transition of the neutral-state CPs.

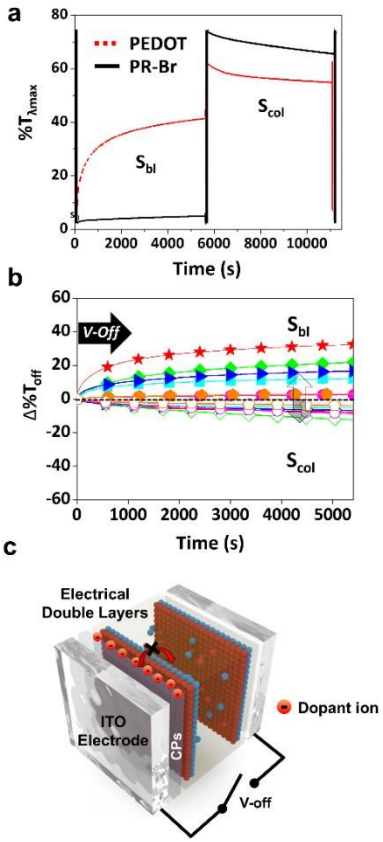

Fig. 3 (a) The transmittance change for S_{bl} and S_{col} at V-Off of the ECW for the PEDOT (dotted red line) and PR-Br (solid black line) films in BIL and monitored at λ_{max}. (b) $\Delta\%T_{off}$ in the colored (S_{bl}, closed symbols) and bleached state (S_{col}, open symbols) for PEDOT (red star), PE-Cl (green diamond), PR-Me (blue triangle), PR-MeO (cyan square), PR-Br (magenta circle), and PR-EHO (orange pentagon). (c) A schematic diagram of the interfacial dopant ion transport (IDT) in BIL for S_{col}.

the CPs (high-E_{HOMO}) upon interface formation according to the integer charge-transfer (ICT) model.[32] However, when the E_F of the electrode is higher than the E_{HOMO} of the CP film (low-E_{HOMO}), such an electron transfer is unfavourable in the colored state (Fig. S10, ESI†).[33] Therefore, the CPs with a higher E_{HOMO} than E_F of the electrode (-4.7eV) should undergo IET, whereas those with a lower E_{HOMO} stay intact in the colored state. Indeed, this analysis agrees well with the experimental result, confirming the long OM for the CPs that have a low E_{HOMO} or high E^p_{ox} (PR-Br and PR-EHO). Thus, the IET is an exclusive controller for the OM in the colored states (Fig. 2b and c, and Table S1, ESI†). Morphology of CP films has been an important factor for the charge/discharge processes that are associated with the EC properties.[31, 34] However, the average roughness (R_a) of the EC films did not correlate with the optical bistability (Fig. S9, ESI†). This result supports the idea that the OM in the colored state can be controlled by the IET.

The two different mechanisms, IET and IDT, can be supported by the kinetic overpotential (η_{kin})[35] leading to self-reactions (S_{bl} and S_{col}) at V-Off as follows :

$$\eta_{kin} = -\frac{(E_{F,p} - E_{pol})}{e} = -\frac{\left(E_{F,p} - E_{\frac{1}{2}} - \frac{RT}{nF} ln\left(\frac{f}{1-f}\right)\right)}{e} \quad (2)$$

where $E_{F,p}$ represents the E_F pinning position at the ITO/CP films interface, and E_{pol} is the energy level of the polymer, as determined by the Nernst equation, [36] which describes the shift in the energy level as a function of the fraction of the oxidized polymer (*f*). The n represents the number of electrons transferred from the EC film to the ITO electrode. R is the universal gas constant, T is the absolute temperature, and F is the Faraday constant. Because the fraction of the oxidized polymer is related to the changes in optical density (ΔOD), the following equation was elucidated to analyze the loss of OM.

$$\Delta OD = \frac{\Delta Abs}{L} = \varepsilon \Delta c \approx \varepsilon \Delta Q \quad (3)$$

The ΔOD is proportional to the total amount of injected/ejected charge during the self-reaction. Thus, the fraction of the oxidized polymer (*f*) generated by the given oxidation charge (Q_{oxi}) was derived from the transmittance (Equation (4)).

$$f = \frac{Q_{oxi}}{Q_{total}} = \frac{Q_{total}(logT_t - logT_{min})}{Q_{oxi}(logT_{max} - logT_{min})} \quad (4)$$

$$CE = \frac{\log\left(\frac{T_{max}}{T_{min}}\right)}{\frac{Q_{total}}{A}};\ Q_{total} = \frac{\log\left(\frac{T_{max}}{T_{min}}\right) \cdot A}{CE};\ Q_{oxi} = \frac{\log\left(\frac{T_t}{T_{min}}\right) \cdot A}{CE} \quad (5)$$

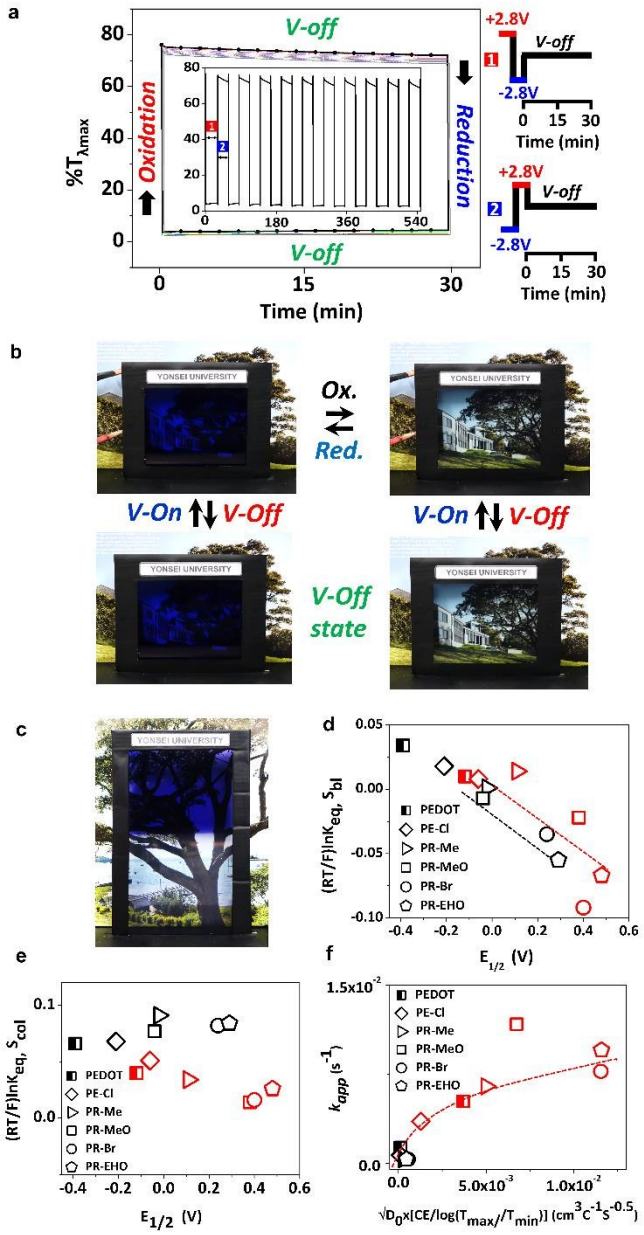

Fig. 4 (a) The bistability of the ECW with PR-Br in BIL under the IET and IDT controlled condition upon alternative switching between step potentials (±2.8 V) at V-Off. (b) Photographic images of the ECW with PR-Br in the colored and bleached state (±2.8 V) at V-Off. (c) Photographic images of the large-area ECW (7 inch) with PR-Br at colored (top) and the transparent (bottom) state at V-off. (d) A plot of $\frac{\mathrm{RT}}{\mathrm{F}}\ln K_{eq}$ as a function of $E_{1/2}$ of the CPs for S_{bl} and (e) for S_{col} of the ECW using TBAP (red symbol) and BIL (black symbol). (f) A plot of the k_{app} as a function of the $\sqrt{D_0}$ of the ECW using TBAP (red symbol) and BIL (black symbols) for PEDOT (half-filled square), PE-Cl (diamond), PR-Me (triangle), PR-MeO (square), PR-Br (circle), and PR-EHO (pentagon).

where T_{min} and T_{max} are the minimum and maximum transmittance, respectively, when the CP films are fully switched. *A* is the area of the CP films. T_t is the transmittance at V-Off at a certain time and Q_{total} is the total injected/ejected charge required to generate a fully reduced or oxidized state. CE is coloration efficiency ($cm^2\,C^{-1}$). Q_{total} and Q_{oxi} can be represented to Equation (5).

Equation (2) can be rearranged to equation (6) by using Equations (4) and (5).

$$\eta_{kin} = -\frac{\left(E_{F,p} - E_{1/2} - \frac{\mathrm{RT}}{\mathrm{nF}}\ln\left(\frac{Q_{total}(logT_t - logT_{min})}{Q_{oxi}(logT_{max} - logT_{min})}\right)\right)}{e} \quad (6)$$

When the transmittance change reaches an equilibrium state, Equation (6) can be represented by Equation (7).

$$\eta_{kin} = -\frac{\left(E_{F,p} - E_{1/2} - \frac{\mathrm{RT}}{\mathrm{nF}}\ln K_{eq}\right)}{e} \quad (7)$$

The interfacial electron transfer continues until it reaches an equilibrium between $E_{F,p}$ and E_{pol}. When the $\Delta\%T_{off}$ reaches an equilibrium state, $\frac{\mathrm{RT}}{\mathrm{F}}\ln K_{eq}$ is directly related to $E_{1/2}$ during the self-reaction (Equation (7)). This showed roughly a linear relationship between $\frac{\mathrm{RT}}{\mathrm{F}}\ln K_{eq}$ and $E_{1/2}$ for S_{bl} (Fig. 4d), indicating that $\Delta\%T_{off}$ becomes smaller when E^{p}_{ox} becomes larger (Fig. S12, ESI†). Thus, the OM in the colored state should be long with CPs that have a low E_{HOMO}. However, there is no linear relationship for S_{col} (Fig. 4e), indicating that the S_{col} process was not fully controlled by the IET. S_{col} should be energetically favorable for all polymers because of the small localized band gap energy.[37] Under this condition, any small driving force, such as the blocking of ion diffusion or transfer, will distract S_{col}.

Because the doped-state CPs can be considered to be positively charged CP films that are in contact with the dopant anions, the dopant ion concentration difference between the CP films and the electrolyte interface can generate a diffusion potential (η_{diff}). The diffusion potential, which is due to the anion concentration difference, can be obtained from the following Equation (8):

$$\eta_{diff} = -\frac{(E_{pol} - E_s)}{e} = \frac{RT}{F}\ln\frac{(a_{A^-})_{pol}}{(a_{A^-})_s} \quad (8)$$

where E_S represents the energy level of the electrolyte and $(a_{A^-})_{pol}$ and $(a_{A^-})_s$ represent the activities of the anions in the CP films and electrolytes, respectively. For a diffusion controlled electrochemical reaction, the diffusion current (i_d) is described by the Cottrell equation (Equation (9)):

$$i_d(\mathrm{t}) = \frac{nFAD_0^{\frac{1}{2}}}{\sqrt{\pi \mathrm{t}}}\left([pol^+ \cdot A^-]_{pol} - [A^-]_s\right) = \frac{nFAD_0^{\frac{1}{2}}}{\sqrt{\pi \mathrm{t}}}\left([a_{A^-}]_{pol} - [a_{A^-}]_s\right) \quad (9)$$

where F is the Faraday constant, A is the reacted area of the CPs, D_0 is the diffusion coefficient, t is the time, and $[A^-]_s$ is the counter ion of the electrolyte that is injected/ejected to maintain the electro-neutrality inside the CP films. $[Pol^+ \cdot A^-]_{pol}$ represents the bleached state that has a counter ion for balancing. The consumed charge (Q_d) could be derived from $i_d(\mathrm{t})$ (Equation (10)):

$$Q_d(\mathrm{t}) = 2\frac{nFAD_0^{\frac{1}{2}}}{\sqrt{\pi}}(\,[a_{A^-}]_{pol} - [a_{A^-}]_s) \times \sqrt{\mathrm{t}} \quad (10)$$

The relationship between the transmittance change and the diffusion coefficient can be derived as follows. From the CE (Equation (5)), the fraction of the electrochemically changed polymer (*f*) can be represented by Equation (11):

$$1 - f = \frac{Q_d(t)}{\mathrm{Q}_{total}} = \frac{Q_d(t) \times \mathrm{CE}}{\log(\frac{T_{max}}{T_{min}})A} \quad (11)$$

$$1 - f = \frac{Q_d(t)}{\mathrm{Q}_{total}} = 1 - \frac{logT_t - logT_{min}}{logT_{max} - logT_{min}} = k_{app}\sqrt{\mathrm{t}} \quad (12)$$

The apparent rate constant (k_{app}) was determined from the slope of fitting *f* and the square root of time with Equation (12) (Table S4).
The *f* and square root of time fitting for S_{col} was determined from the Fig. S3 data within 500 s (Fig. S13).
Fig. 4f clearly displays that the self-coloring process is diffusion controlled in TBAP. The k_{app} for S_{col} is proportional to the diffusion term ($\sqrt{D_0}$) in TBAP. However, all of the k_{app} in BIL were very low and almost invariant to the $\sqrt{D_0}$ values for different polymers, regardless of their large variations of E_{HOMO}. This low k_{app} for S_{col} could be attributed to the EDL. Therefore, the OM in the bleached state was significantly enhanced in BIL.

Conclusions

In summary, a low E_{HOMO} level CP films afforded an energy saving bistable ECW by controlling the interfacial charge transport. The mechanism for self-bleaching was ascribed to the electron transfer between the ITO and the CPs (IET), which was supported by correlating the $\Delta\%T_{off}$ with the E^p_{ox} of the polymers at V-Off. The self-coloring process in the ECWs was explained by the ion transfer from the CPs to the electrolytes (IDT), which was blocked by the EDL, providing a long bistability for the CPs with low E_{HOMO}. These two different mechanisms for the OM in self-bleaching (IET) and self-coloring (IDT) were supported by the energy level and diffusion term, respectively. The ECW from the new CPs (PR-Br) maintained the OM for 90 min at V-Off with a large $\Delta\%T_{\lambda max}$ (> 70%). This allowed the first preparation of a high contrast, fast-switching, and energy-saving ECW.

Acknowledgements

We acknowledge the financial support of the National Research Foundation (NRF) grant funded by the Korean government (Ministry of Science, ICT & Future Planning, MSIP) through the Active Polymer Center for Pattern Integration (APCPI) (2007–0056091). This work was also supported by The Next-generation Converged Energy Material Research Center (CEMRC) of Agency for Defense Development (ADD).

Notes and references

1 C. Park, S. Seo, H. Shin, B. D. Sarwade, J. Na and E. Kim, *Chem. Sci.*, 2015, **6**, 596.
2 J. Kim, G. K. Ong, Y. Wang, G. LeBlanc, T. E. Williams, T. M. Mattox, B. A. Helms and D. J. Milliron, *Nano Lett.*, 2015, **15**, 5574.
3 G. Tsekouras, N. Minder, E. Figgemeier, O. Johansson and R. Lomoth, *J. Mater. Chem.*, 2008, **18**, 5824.
4 H. W. Heuer, R. Wehrmann and S. Kirchmeyer, *Adv. Funct. Mater.*, 2002, **12**, 89.
5 A. Llordes, G. Garcia, J. Gazquez and D. J. Milliron, *Nature*, 2013, **500**, 323.
6 J. Kim, J. You, B. Kim, T. Park and E. Kim, *Adv. Mater.*, 2011, **23**, 4168.
7 K. Krishnamoorthy, A. V. Ambade, M. Kanungo, A. Q. Contractor and A. Kumar, *J. Mater. Chem.*, 2001, **11**, 2909.
8 D. M. Welsh, A. Kumar, E. W. Meijer and J. R. Reynolds, *Adv. Mater.*, 1999, **11**, 1379.
9 S. Papaefthimiou, *Adv. Building Energy Res.*, 2010, **4**, 77.
10 P. M. Beaujuge and J. R. Reynolds, *Chem. Rev.*, 2010, **110**, 268.
11 C. X. Dai Ning, Lu Liu, Calen Kaneko, Minoru Taya, *Proceeding of SPIE*, 2005, **5759**, 260.
12 V. K. Thakur, G. Ding, J. Ma, P. S. Lee and X. Lu, *Adv. Mater.*, 2012, **24**, 4071.
13 J. Padilla, V. Seshadri, J. Filloramo, W. K. Mino, S. P. Mishra, B. Radmard, A. Kumar, G. A. Sotzing and T. F. Otero, *Synth. Met.*, 2007, **157**, 261.
14 Y. Zhu, M. T. Otley, F. A. Alamer, A. Kumar, X. Zhang, D. M. D. Mamangun, M. Li, B. G. Arden and G. A. Sotzing, *Org. Electron.*, 2014, **15,** 1378.
15 E. M. Girotto and M.-A. De Paoli, *J. Brazil. Chem. Soc.*, 1999, **10**, 394.
16 M. O. M. Edwards and R. Persson, *J. Soc. Infor. Display*, 2005, **13**, 1035.
17 H. Ishii, K. Sugiyama, E. Ito and K. Seki, *Adv. Mater.*, 1999, **11**, 605.
18 N. Koch, A. Kahn, J. Ghijsen, J.-J. Pireaux, J. Schwartz, R. L. Johnson and A. Elschner, *Appl. Phys. Lett.*, 2003, **82**, 70.
19 W. Lu, A. G. Fadeev, B. Qi, E. Smela, B. R. Mattes, J. Ding, G. M. Spinks, J. Mazurkiewicz, D. Zhou, G. G. Wallace, D. R. MacFarlane, S. A. Forsyth and M. Forsyth, *Science*, 2002, **297**, 983.
20 P. M. Beaujuge, S. Ellinger and J. R. Reynolds, *Nature Mater*, 2008, **7**, 795.
21 D. M. Welsh, L. J. Kloeppner, L. Madrigal, M. R. Pinto, B. C. Thompson, K. S. Schanze, K. A. Abboud, D. Powell and J. R. Reynolds, *Macromolecules*, 2002, **35**, 6517.
22 L. Groenendaal, F. Jonas, D. Freitag, H. Pielartzik and J. R. Reynolds, *Adv. Mater.*, 2000, **12**, 481.
23 J. Roncali, *Chem. Rev.*, 1997, **97**, 173.
24 J. Roncali, *Macromol. Rapid Commun.*, 2007, **28**, 1761.
25 D. M. Welsh, A. Kumar, M. C. Morvant and J. R. Reynolds, *Synth. Met.*, 1999, **102**, 967.
26 B. D. Reeves, C. R. G. Grenier, A. A. Argun, A. Cirpan, T. D. McCarley and J. R. Reynolds, *Macromolecules*, 2004, **37**, 7559.
27 S. Zhong, J. Q. Zhong, H. Y. Mao, J. L. Zhang, J. D. Lin and W. Chen, *Phys. Chem. Chem. Phys.*, 2012, **14**, 14127.
28 T. Fujimoto and K. Awaga, *Phys. Chem. Chem. Phys.*, 2013, **15**, 8983.
29 K. Kirchner, T. Kirchner, V. Ivaništšev and M. V. Fedorov, *Electrochim. Acta*, 2013, **110**, 762.

30 S. Perkin, L. Crowhurst, H. Niedermeyer, T. Welton, A. M. Smith and N. N. Gosvami, *Chem. Commun.*, 2011, **47**, 6572.
31 J.-H. Huang, C.-Y. Hsu, C.-W. Hu, C.-W. Chu and K.-C. Ho, *ACS Appl. Mater. Interfaces*, 2010, **2**, 351.
32 S. Braun, W. R. Salaneck and M. Fahlman, *Adv. Mater.*, 2009, **21**, 1450.
33 M. Atobe, S. Inagi and T. Fuchigami, *Fundamentals and Applications of Organic Electrochemistry [electronic resource] : Synthesis, Materials, Devices*, Hoboken : Wiley, Hoboken, 2014.
34 Y. Kim, Y. Kim, S. Kim and E. Kim, *ACS Nano*, 2010, **4**, 5277.
35 R. Reineke and R. Memming, *J. Phys. Chem.*, 1992, **96**, 1317.
36 L. R. Faulkner and A. J. Bard, *Electrochemical methods : fundamentals and applications*, New York : John Wiley & Sons, New York, 2001.
37 O. Bubnova and X. Crispin, *Energy Environ. Sci.*, 2012, **5**, 9345.

